Quantum-phase dynamics of an atomic/molecular system interacting with a two-mode squeezed vacuum field: Coexistence of quantum and thermal features

ARTICLE *in* CHEMICAL PHYSICS · JANUARY 2003

Impact Factor: 1.65 · DOI: 10.1016/S0301-0104(02)00918-7

2 AUTHORS, INCLUDING:

Masayoshi Nakano
Osaka University
337 PUBLICATIONS **4,781** CITATIONS

Available online at www.sciencedirect.com
SCIENCE DIRECT®
Chemical Physics 286 (2003) 257–266
Chemical Physics
www.elsevier.com/locate/chemphys

Quantum-phase dynamics of an atomic/molecular system interacting with a two-mode squeezed vacuum field: coexistence of quantum and thermal features

Masayoshi Nakano*, Kizashi Yamaguchi

Department of Chemistry, Graduate School of Science, Osaka University, Toyonaka, Osaka 560-0043, Japan

Received 22 April 2002

Abstract

We investigate the dynamics of a three-state atomic/molecular model system interacting with a two-mode squeezed vacuum field in view of the correlation between the atomic/molecular density matrix and photon-phase distribution. It is found that two-mode squeezed vacuum field realizes the anomalous situation that the coherency between the atomic/molecular states concerning the two-photon process is preserved well during the dynamics though the coherency between other states completely vanish. This implies that the quantum and thermal features can coexist in the atomic/molecular system in the presence of two-mode squeezed vacuum field. Such phenomenon is found to originate in the feature of its initial photon-phase correlation of a two-mode squeezed vacuum. We also discuss how the present attractive features in off-diagonal density matrices affect the molecular non-linear polarization.

1. Introduction

Quantum features of the population dynamics for atoms/molecules under quantized photon fields with various quantum statistics have generated considerable interest not only in quantum optics but also in atomic/molecular science [1–4]. The simplest model of such problems is the Jaynes–Cummings (JC) model [5], which describes the interaction between a two-state atom and a one-mode photon field. The result of this dynamics provides purely quantum features, e.g., collapse, quiescence and revival behavior of the Rabi oscillations [6], which cannot be caused by conventional laser fields. The mechanism of the collapse-revival behavior was found to originate in the dephasing and rephasing among the Rabi oscillations with slightly different frequencies [6]. Although these attractive features were predicted theoretically at first, recent experiments support some of these effects [7,8]. A recent direction of the extension of the JC model is the consideration of the interaction between atoms/molecules and two-mode photon fields. In general, there are two types of two-mode

* Corresponding author.
E-mail address: mnaka@chem.sci.osaka-u.ac.j (M. Nakano).

0301-0104/03/$ - see front matter
PII: S0301-0104(02)00918-7

fields, i.e., initially uncorrelated and correlated two-mode fields. Many studies on the dynamics of a three-state atom interacting with an uncorrelated two-mode field, e.g., two-mode thermal (chaotic) and two-mode coherent fields, have been carried out and have elucidated the feature of the dynamics from the viewpoint of the intermode field correlation [9,10]. There are also studies on the effect of initial intermode field correlations of two-mode squeezed vacuum field [11] on the population dynamics of the system [10]. The two-mode squeezed vacuum field is a highly non-classical state of the photon field in which the individual modes display random thermal fluctuations though a superposition of the modes exhibits a reduction in noise below the quantum limit [12]. It was found that the population dynamics of atoms/molecules under a two-mode squeezed vacuum field is similar to that of the two-mode thermal field though the amplitudes of Rabi oscillations for the two-mode squeezed vacuum field are somewhat larger than those for the two-mode thermal field [10]. On the other hand, there have been few studies on the dynamics of quantum-phase properties of two-mode photon fields by means of the Pegg and Barnett (PB) phase operator [13], which is expected to provide a profound insight into the quantum coherency in such dynamics. In this study, therefore, we numerically examine the dynamical behavior of the PB photon-phase distributions and the off-diagonal atomic/molecular density matrices, which represent the relative-phase (coherency) dynamics between electronic states of the atom/molecule, for coupled systems composed of a three-state molecular model and a two-mode squeezed field, i.e., a two-mode squeezed vacuum field or a two-mode squeezed coherent field. In comparison of these results with those of two-mode thermal and two-mode coherent fields, we elucidate the relations between the dynamics of on- and off-diagonal atomic/molecular density matrices and that of photon-phase distributions. Finally, we present a possible method of elucidating the effects of the dynamical features of the off-diagonal density matrices under a two-mode squeezed vacuum on non-linear optical response properties, which directly relate to observed phenomena.

2. Calculation method and model system

2.1. Hamiltonian for a coupled system composed of an atom/molecule and a two-mode photon field

The three-state model (Fig. 1) considered in this study mimics the electronic states of *trans*-octatetraene, which is a typical π-conjugated linear chain system. It is found from the PPP-full-configuration-interaction (PPP-FCI) calculation [14] that the molecular energy intervals are $E_{21}(\equiv E_2 - E_1) = 36\,791\ \mathrm{cm}^{-1}$ and $E_{32}(\equiv E_3 - E_2) = 21\,864\ \mathrm{cm}^{-1}$, and that the transition moments in the chain-length direction are $d_{21} = 8.454$ D and $d_{32} = 14.362$ D. We consider two photon frequencies ($\omega_1 = 36\,791\ \mathrm{cm}^{-1}$ and $\omega_2 = 21\,864\ \mathrm{cm}^{-1}$), which are resonant with E_{21} and E_{32}, respectively. It is noted that the results obtained in this study can be applied to more general three-state models though we use a specific model. The Hamiltonian used is given in Eq. (1). The first, the second and the third terms on the right side of Eq. (1) represent the unperturbed atomic/molecular

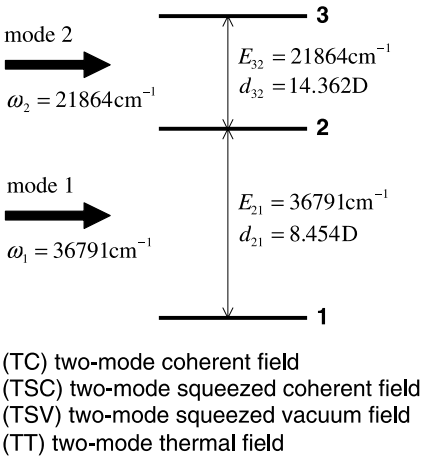

Fig. 1. Three-state model interacting with a two-mode photon field. The ω_1 and ω_2 are frequencies which are resonant with the energy intervals $E_{21} = 36\,791\ \mathrm{cm}^{-1}$ and $E_{32} = 21\,864\ \mathrm{cm}^{-1}$, respectively. The transition moments are $d_{21} = 8.454$ D and $d_{32} = 14.362$ D. We consider three types of photon fields, i.e., two-mode coherent field (TC), two-mode squeezed coherent field (TSC) ($r = 1.0$ and $\varphi = 0$), two-mode squeezed vacuum field (TSV) and two-mode thermal field (TT). The initial average photon number of each mode of these fields is 4.

system, the two-mode photon field and their interaction, respectively:

$$H = \sum_{i}^{3} E_i a_i^+ a_i + \sum_{\lambda}^{2} \left(b_\lambda^+ b_\lambda + \frac{1}{2} \right) \hbar\omega_\lambda + \sum_{i,j}^{3} \sum_{\lambda}^{2} \left(\frac{\hbar\omega_\lambda}{2\varepsilon_0 V} \right) d_{ij} a_i^+ a_j (b_\lambda^+ + b_\lambda). \quad (1)$$

In the first term, E_i represents the energy of the atomic/molecular state i, and a_i^+ and a_i are, respectively, the creation and annihilation operators for the quantized electron field in the ith energy state. In the second term, ω_λ indicate the frequency of photon mode λ, and b_λ^+ and b_λ are the creation and annihilation operators for photon mode λ. In the third term, d_{ij} is the matrix element of the atomic/molecular dipole moment operator in the direction of the polarization of photon field. It is assumed that the polarization vector of each mode coincides with each other. V is the volume of the cavity containing the one-mode photon field, and it is fixed to 10^7 Å^3 in this study. It is noted that V is related to the coupling between an atom/molecule and the two-mode photon field and thus affects the time scale of collapse-revival behaviors. Namely, the qualitative results obtained in this study will be observed in alternative systems with different parameters, E_i, ω_λ, V, d_{ij} and $\langle n_\lambda \rangle$ (initial average photon number). In the case of a molecule, we neglect the couplings between electronic states and nuclear vibrations in this model. Such approximate model can be acceptable for either the case where the time intervals considered are much faster than any change of nuclear configuration of the molecule or the case where the couplings between electrons and nuclear motions are much smaller than other couplings. The matrix elements of the above Hamiltonian are obtained by using a triple Hilbert space spanned by the atomic/molecular states $\{|j\rangle\}$ $(j = 1, 2, 3)$ and the photon-number states of modes 1 and 2, i.e., $\{|n_1\rangle\}$ and $\{|n_2\rangle\}$ $(n_1, n_2 = 0, 1, 2, \ldots, \infty)$. Namely, the triple Hilbert space basis consists of the states $|j; n_1, n_2\rangle$ $(\equiv |j\rangle \otimes |n_1\rangle \otimes |n_2\rangle)$. In numerical calculations, we use $n_1, n_2 = 0, 1, \ldots, 14$ as the size of truncated Hilbert space, which is sufficient for obtaining converged results for our purpose.

2.2. Procedure of dynamics of atom/molecule-photon coupled system

Using the eigenvalues $\{W(m)\}$ and eigenvectors $\{\chi(m)\}$ $(m = 0, 1, 2, \ldots)$ of the Hamiltonian (Eq. (1)), the matrix element of the time-evolution operator is written by

$$\begin{aligned} &\langle j; n_1, n_2 | U(t, t_0) | j'; n_1', n_2' \rangle \\ &\quad \equiv U_{j,n_1,n_2;j',n_1',n_2'} \\ &\quad = \sum_m \langle j; n_1, n_2 | \chi(m) \rangle \langle \chi(m) | j'; n_1', n_2' \rangle \mathrm{e}^{-\mathrm{i}W(m)(t-t_0)/\hbar}. \end{aligned} \quad (2)$$

The elements of density matrix are represented by

$$\begin{aligned} &\langle j; n_1, n_2 | \rho(t) | j'; n_1', n_2' \rangle \\ &\quad \equiv \rho_{j,n_1,n_2;j',n_1',n_2'}(t) \\ &\quad = \sum_{f,g}^{3} \sum_{\substack{m_1,m_2, \\ m_1',m_2'}} U_{j,n_1,n_2;f,m_1,m_2}(t, t_0) \rho_{f,m_1,m_2;g,m_1',m_2'}(t_0) \\ &\qquad \times U^+_{g,m_1',m_2';j',n_1',n_2'}(t, t_0). \end{aligned} \quad (3)$$

The procedure of dynamics is described as follows. Firstly, we construct an initial density matrix $(\rho_{f,m_1,m_2;g,m_1',m_2'}(t_0))$, which can be separated into the product of an atomic/molecular density matrix $(\rho^{\mathrm{mol}}_{f,g}(t_0))$ and a two-mode photon density matrix $(\rho^{\mathrm{2phot}}_{m_1,m_2;m_1',m_2'}(t_0))$. The atom/molecule is assumed to be in the ground state at the initial time. As the initial field state, we consider four types of two-mode field states with the same averaged photon number $(\langle \hat{n}_1 \rangle = \langle \hat{n}_2 \rangle = 4)$, i.e., a two-mode coherent (TC), a two-mode squeezed coherent (TSC), a two-mode squeezed vacuum (TSV) and a two-mode thermal (TT) field states. The (TC) and (TT) are uncorrelated two-mode fields, so that their two-mode photon density matrices are constructed by the direct product of the density matrix concerning each one-mode field. The density matrix elements of (TC) are expressed by

$$\rho^{\mathrm{2phot}}_{m_1,m_2;m_1',m_2'} = \langle m_1, m_2 | \beta_1, \beta_2 \rangle \langle \beta_1, \beta_2 | m_1', m_2' \rangle, \quad (4)$$

where $|\beta_1, \beta_2\rangle$ represents (TC) expressed by

$$|\beta_1,\beta_2\rangle = \exp\left[-\frac{1}{2}(|\beta_1|^2+|\beta_2|^2)\right] \times \sum_{n_1}^{\infty}\sum_{n_2}^{\infty}\frac{\beta_1^{n_1}}{\sqrt{n_1!}}\frac{\beta_2^{n_2}}{\sqrt{n_2!}}|n_1,n_2\rangle. \quad (5)$$

Here, $\{\beta_\lambda\}$ is the eigenvalue of annihilation operator b_λ for photon mode λ with the eigenvector (coherent state) $\{|\beta_\lambda\rangle\}$. The density matrix elements of (TT) are expressed by

$$\rho^{\text{2phot}}_{m_1,m_2;m_1',m_2'} = \frac{\langle\hat{m}_1\rangle^{m_1}}{(1+\langle\hat{m}_1\rangle)^{m_1+1}} \times \frac{\langle\hat{m}_2\rangle^{m_2}}{(1+\langle\hat{m}_2\rangle)^{m_2+1}}\delta_{m_1m_1'}\delta_{m_2m_2'}, \quad (6)$$

where $\hat{m}_\lambda$ is the photon-number operator defined by $\hat{m}_\lambda \equiv b_\lambda^+ b_\lambda$. It is noted that the thermal field has no off-diagonal elements, the feature of which indicates that the thermal field is a mixed state and has no definite phase relation between each photon-number state. In contrast to these fields, (TSC) and (TSV) are correlated two-mode fields, so that they cannot be represented by the direct product of each one-mode density matrix. For two modes 1 and 2 with annihilation operators b_1 and b_2, (TSC) (represented by $|\beta_1,\beta_2;\zeta\rangle$) is unitarily related to vacuum state $|0,0\rangle$ (the ground state of the two-mode photon field) by the action of two-mode displacement operator ($\hat{D}(\beta_1,\beta_2)\equiv\hat{D}(\beta_1)\hat{D}(\beta_2)$) and two-mode squeezing operator ($\hat{S}_{12}(\zeta)$) in the following manner [15–20]:

$$|\beta_1,\beta_2;\zeta\rangle = \hat{D}(\beta_1,\beta_2)\hat{S}_{12}(\zeta)|0,0\rangle, \quad (7)$$

where

$$\hat{D}(\beta_\lambda) = \exp(\beta_\lambda b_\lambda^+ - \beta_\lambda^* b_\lambda) \quad (\lambda=1,2), \quad (8)$$

and

$$\hat{S}_{12}(\zeta) = \exp(\zeta^* b_1 b_2 - \zeta b_1^+ b_2^+). \quad (9)$$

Here, $\zeta = re^{i\varphi}$ is any complex number with modulus r and argument φ, which determine the squeezing intensity and the direction of squeezing, respectively. Two-mode squeezing arises in models of two-photon non-linear optics being associated with non-degenerate process, where pairs of photons are generated, one in each of modes 1 and 2, by the action of $b_1^+ b_2^+$. In this study, β_1 is equal to β_2, and we use $r=1.0$ and $\varphi=0$ for (TSC), in the case of which photons between modes 1 and 2 are antibunched with each other due to the second-order cross-correlation $g_{12}^{(2)}$ ($=0.608$) <1. In particular, (TSV), $|0,0;\zeta\rangle$ ($\equiv\hat{S}_{12}(\zeta)|0,0\rangle$), is given by [21]

$$|0,0;\zeta\rangle = \text{sech}r\sum_n[-\exp(i\varphi)\tanh r]^n|n_1;n_2\rangle. \quad (10)$$

This field state is a superposition only of states in which the two modes contain the same number of photons. It is also noted that the one-mode properties of each of (TSV) are precisely those of a one-mode thermal field state [21]. The relation between the average photon number of each mode and squeezing (r) parameters for (TSC) and (TSV) is represented by

$$\langle\hat{n}_\lambda\rangle - |\sinh r|^2 = |\beta_\lambda|^2 \geqslant 0 \quad (\lambda=1,2). \quad (11)$$

The density matrix elements of (TSC) and (TSV) are obtained by $\rho^{\text{2phot}}_{m_1,m_2;m_1',m_2'} = \langle m_1,m_2|\beta_1,\beta_2;\zeta\rangle\langle\beta_1,\beta_2;\zeta|m_1',m_2'\rangle$ using Eqs. (7)–(10). Secondly, the density matrix elements ($\rho_{j,n_1,n_2;j',n_1',n_2'}(t)$) at time t are calculated using Eq. (3). Thirdly, several reduced density matrix elements are calculated by

$$\rho^{\text{mol}}_{f,g}(t) = \sum_{m_1,m_2}\rho_{f,m_1,m_2;g,m_1,m_2}(t)$$

(atomic/molecular density), (12)

$$\rho^{\text{2phot}}_{m_1,m_2;m_1',m_2'}(t) = \sum_f \rho_{f,m_1,m_2;f,m_1',m_2'}(t)$$

(two-mode photon-field density), (13)

$$\rho^{\text{1phot}}_{m_1,m_1'}(t) = \sum_{m_2}\rho^{\text{2phot}}_{m_1,m_2;m_1',m_2}(t)$$

(one-mode photon-field density for mode 1), (14)

and

$$\rho^{\text{1phot}}_{m_2,m_2'}(t) = \sum_{m_1}\rho^{\text{2phot}}_{m_1,m_2;m_1,m_2'}(t)$$

(one-mode photon-field density for mode 2). (15)

Finally, various properties concerning the atom/molecule and photons are calculated using these reduced density matrices.

2.3. Two-mode Pegg–Barnett (PB) phase operator

After Pegg and Barnett introduced a Hermitian phase operator [13], the phase properties of various photon fields and molecule-photon field coupled systems have been investigated [2–4,22]. They also extended their theory to analyze the phase properties of pairs of photon fields [21]. In this section, we briefly explain their two-mode PB phase operator for the analysis of the phase dynamics of the atom/molecule-photon coupled systems considered in this study.

In the PB approach, all calculations concerning the phase properties are performed in an $(s+1)$-dimensional space spanned by $s+1$ orthonormal phase states, and the s value will be taken to be infinity after all the expectation values have been calculated. The $s+1$ orthonormal phase states of a one-mode field are defined by

$$|\phi_m\rangle = \frac{1}{(s+1)^{1/2}} \sum_n^s \mathrm{e}^{\mathrm{i}n\phi_m}|n\rangle, \tag{16}$$

where $\phi_m = \phi_0 + 2\pi m/(s+1)$ $(m = 0, 1, 2, \ldots, s)$ and ϕ_0 is an arbitrary real number. In this study, s is taken to be 100 and we adopt $\phi_0 = -s\pi/(s+1)$ to locate the initial phase of a one-mode coherent photon field on the origin ($\phi = 0$) of the phase axis defined in the region: $-\pi \leqslant \phi_m \leqslant \pi$. In the case of a two-mode field, these relations are satisfied for each mode field.

Pegg and Barnett defined the following Hermitian phase operator of mode λ to provide the eigenvalues $\{\phi_m^\lambda\}$ and the eigenstates $\{|\phi_m^\lambda\rangle\}$.

$$\hat{\phi}^\lambda = \sum_m^s \phi_m^\lambda |\phi_m^\lambda\rangle\langle\phi_m^\lambda|. \tag{17}$$

Based on this definition, we can calculate the expectation values of arbitrary continuous functions of the two-mode phase operator ($f(\hat{\phi}^1, \hat{\phi}^2)$). By using the PB operator, the operator $f(\hat{\phi}^1, \hat{\phi}^2)$ can be defined as

$$\begin{aligned} f(\hat{\phi}^1, \hat{\phi}^2) &= f\left(\sum_{m_1}^s \phi_{m_1}^1 |\phi_{m_1}^1\rangle\langle\phi_{m_1}^1|, \sum_{m_2}^s \phi_{m_2}^2 |\phi_{m_2}^2\rangle\langle\phi_{m_2}^2|\right) \\ &= \sum_{m_1,m_2}^s f(\phi_{m_1}^1, \phi_{m_2}^2)|\phi_{m_1}^1\rangle|\phi_{m_2}^2\rangle\langle\phi_{m_1}^1|\langle\phi_{m_2}^2|. \end{aligned} \tag{18}$$

The expectation values of $f(\hat{\phi}^1, \hat{\phi}^2)$ for arbitrary physical states $|\psi\rangle$ can be calculated by

$$\begin{aligned} \langle f(\hat{\phi}^1, \hat{\phi}^2)\rangle &= \lim_{s\to\infty} \langle\psi|f(\hat{\phi}^1, \hat{\phi}^2)|\psi\rangle \\ &= \lim_{s\to\infty} \sum_{m_1,m_2}^s f(\phi_{m_1}^1, \phi_{m_2}^2) P(\phi_{m_1}^1, \phi_{m_2}^2), \end{aligned} \tag{19}$$

where $P(\phi_{m_1}^1, \phi_{m_2}^2)$ is the two-mode photon-phase distribution, which represents the joint probability density for phases $\phi_{m_1}^1$ and $\phi_{m_2}^2$. Using Eqs. (13) and (16), the two-mode phase distribution function can be expressed by

$$P(\phi_{m_1}^1, \phi_{m_2}^2) = \frac{1}{(s+1)^2} \sum_{\substack{n_1,n_2,\\ n_1',n_2'}} \rho^{\mathrm{2phot}}_{n_1,n_2;n_1',n_2'} \mathrm{e}^{\mathrm{i}(n_1'-n_1)\phi_{m_1}^1} \mathrm{e}^{\mathrm{i}(n_2'-n_2)\phi_{m_2}^2}. \tag{20}$$

The surface represented by $P(\phi_{m_1}^1, \phi_{m_2}^2)$ is 2π periodic along both ϕ^1 and ϕ^2 axes. Using Eqs. (19) and (20), we calculate various photon-phase properties for molecule-photon field coupled systems at time t. The phase-sum distribution $P(\phi_m^+)(\equiv P(\phi_{m_1}^1 + \phi_{m_2}^2))$ is represented by

$$P(\phi_m^+) = \frac{1}{(s+1)} \sum_{n_1,n_2} \sum_{n_1'} \rho^{\mathrm{2phot}}_{n_1',(n_1'-n_1+n_2);n_1,n_2} \mathrm{e}^{\mathrm{i}(n_1-n_1')\phi_m^+}. \tag{21}$$

The phase-difference distribution $P(\phi_m^-)$ $(\equiv P(\phi_{m_2}^2 - \phi_{m_1}^1))$ is represented by

$$P(\phi_m^-) = \frac{1}{(s+1)} \sum_{n_1,n_2} \sum_{n_1'} \rho^{\mathrm{2phot}}_{n_1',(n_1-n_1'+n_2);n_1,n_2} \mathrm{e}^{\mathrm{i}(n_1'-n_1)\phi_m^-}. \tag{22}$$

3. Results and discussion

Firstly, we investigate the dynamics of diagonal atomic/molecular density matrix (population) of each state of the molecule for these four types of two-mode fields (Figs. 2(TC-dd), (TSC-dd), (TSV-dd), and (TT-dd)). Apparently, there are two types of Rabi oscillations: one is collapse-revival behavior for (TC) and (TSC) and another is irregular behavior for (TSV) and (TT). (TC) and (TSC) exhibit two types of revival-collapse regions, one of which shows larger amplitudes than the other does, though the collapse time (the time taken for the envelope to collapse to zero) and the revival time (the time taken for the most complete revival of the initial population) for (TC) are different from those for (TSC), respectively. The difference between the first and the second revival-collapse behavior for (TC) are shown to be more distinct than that for (TSC). Also, the irregular Rabi oscillations for (TSV) are found to be larger than those for (TT). This difference is found to be

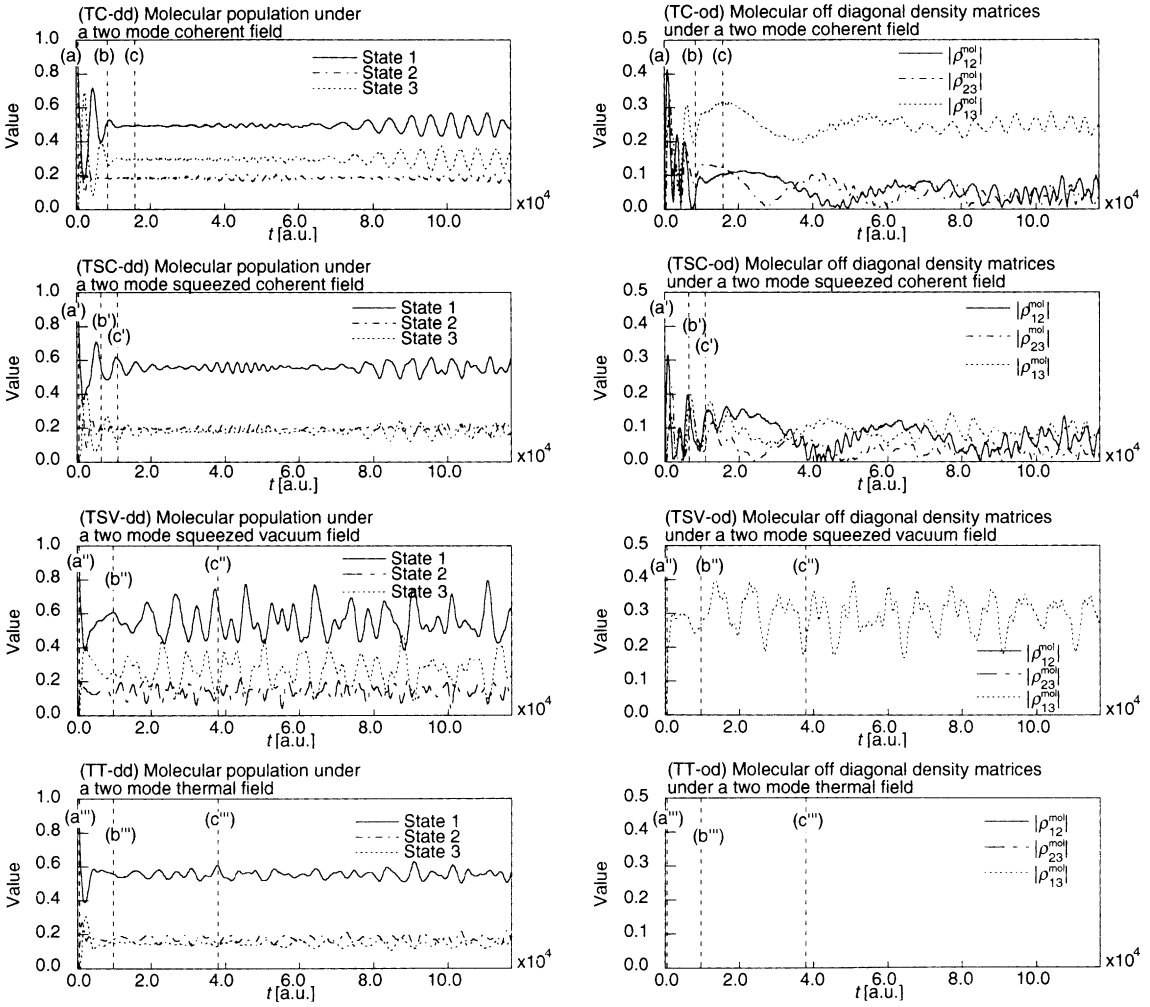

Fig. 2. Time evolution of the population of each state of a three-state atom/molecule for the two-mode coherent field (TC), two-mode squeezed coherent field (TSC), two-mode squeezed vacuum field (TSV) and two-mode thermal field (TT) is shown in (TC-dd), (TSC-dd), (TSV-dd), and (TT-dd), respectively. The dynamics of off-diagonal atomic/molecular density matrices for (TC), (TSC), (TSV), and (TT) is also shown in (TC-od), (TSC-od), (TSV-od), and (TT-od), respectively.

attributed to the initial intermode correlation in (TSV) [10]. Secondly, we investigate the dynamics of off-diagonal molecular density matrices for these four types of two-mode fields (Figs. 2(TC-od), (TSC-od), (TSV-od) and (TT-od)). In contrast to the dynamics of molecular populations, remarkable differences are observed in the dynamics of $|\rho^{\mathrm{mol}}_{1,3}|$ for these four types of two-mode fields. Namely, the $|\rho^{\mathrm{mol}}_{1,3}|$ for (TC) is shown to be much larger than that for (TSC) though the dynamics of other density matrices ($|\rho^{\mathrm{mol}}_{1,2}|$ and $|\rho^{\mathrm{mol}}_{2,3}|$) for (TC) is similar to that for (TSC). The $|\rho^{\mathrm{mol}}_{1,3}|$ for (TSV) are also found to maintain the oscillations with a large averaged value which is similar to that for (TC) though other elements ($|\rho^{\mathrm{mol}}_{1,2}|$ and $|\rho^{\mathrm{mol}}_{2,3}|$) vanish similarly to the case of (TT). As a result, we find remarkable differences in the dynamics of $|\rho^{\mathrm{mol}}_{1,3}|$ between (TSC) and (TC) as well as between (TSV) and (TT) even though the dynamics of atomic/molecular coherencies, $|\rho^{\mathrm{mol}}_{1,2}|$ and $|\rho^{\mathrm{mol}}_{2,3}|$, for (TSC) and (TSV) is similar to that for (TC) and (TT), respectively.

In order to elucidate the cause for such differences in the off-diagonal atomic/molecular density matrices, we investigate the variation in the two-mode photon distributions, i.e., photon-phase-sum ($P(\phi^+)$) and -difference ($P(\phi^-)$) distributions. The distributions $P(\phi^+)$ and $P(\phi^-)$ for these four types of two-mode fields at three times, e.g., (a)–(c) for (TC) shown in Fig. 2, for the first collapse regions are shown in Figs. 3(a)–(c) for (TC), 3(a′)–(c′) for (TSC), 3(a″)–(c″) for (TSV) and 3(a‴)–(c‴) for (TT). There are significant differences in the initial distributions $P(\phi^+)$ and $P(\phi^-)$ for these four types of fields. Although single peaks around $\phi = 0$ are observed in the initial distributions $P(\phi^+)$ and $P(\phi^-)$ both for (TC) and (TSC) (see Fig. 3(a) and (a′)), for (TSC) the distribution peak of $P(\phi^+)$ is found to be much broader than that of $P(\phi^-)$, which is shown to be a single peak with a little broader width than that of (TC). The $P(\phi^-)$ for (TSV) is also found to be a uniform distribution with a constant value which coincides with that for (TT), while the $P(\phi^+)$ for (TSV) exhibits a sharp single peak around $\phi = \pm\pi$ during early time region (a″)–(c″). This feature relates to the fact that the phenomena, e.g., two-photon processes, contributed by two-mode photon density matrices of (TSV) exhibit intermode correlation though the quantities concerning reduced one-mode photon density matrices of (TSV) coincides with those of (TT), in which intermode correlation completely vanishes. It is well-known that the splitting and colliding of the phase peak correspond to the collapse and revival behavior, respectively [1–3,22,23]. The splitting of the phase peak causes the increase in the ability of destroying the relative phase (coherency) between atomic/molecular states, the feature of which leads to the collapse of atomic/molecular populations. Such correspondence is also observed in this system: the original single peak is shown to split into three peaks (see Figs. 3(a)–(c)). The splitting of $P(\phi^+)$ for (TC) is shown to occur faster than that of $P(\phi^-)$. It is noted that the origin in the phase space concerning $P(\phi^-)$ (including the phase ($(\omega_2 - \omega_1)t$) of the free field) moves as the time proceeds since the time t is taken as $2\pi m/(\omega_1 + \omega_2)$ $(m = 0, 1, 2, \ldots)$ in this study. The indistinct splitting and colliding of the broader peak of $P(\phi^+)$ for (TSC) are assumed to cause the longer Rabi oscillations in the first collapse region and the much smaller magnitude of $|\rho^{\mathrm{mol}}_{1,3}|$ for (TSC) as compared to (TC) case (see Figs. 2(TSC-dd), (TC-dd), (TSC-od) and (TC-od)). For (TSV), the shape of the single peak around $\phi = \pm\pi$ is found to be fairly preserved though the splitting and colliding with slight magnitude are found to occur (see Figs. 3(a″)–(c″)). This is presumed to be caused by the fact that in the present model (one- and two-photon resonant model) although only the two-photon process between state 1 and 3 can split the single $P(\phi^+)$ peak at $\phi = \pm\pi$, its contribution is much smaller than those of one-photon processes, which can split a single phase peak (see Fig. 3(a) (TC) for example). In contrast, the $P(\phi^-)$ distribution maintains flat since it is a quantity concerning the one-mode photon density matrices, each of which is resonant with states 1–2 and 2–3, respectively, and its distribution coincides with that of a thermal field. As a result, the well preserved single-peak shape of $P(\phi^+)$ and the uniform distribution of $P(\phi^-)$ for (TSV) lead to the large magnitude of $|\rho^{\mathrm{mol}}_{1,3}|$ and the disappearance of other off-diagonal matrices ($|\rho^{\mathrm{mol}}_{1,2}|$ and $|\rho^{\mathrm{mol}}_{2,3}|$) for (TSV) (see Fig. 2(TSV-od)). In contrast, both $P(\phi^+)$ and $P(\phi^-)$ for

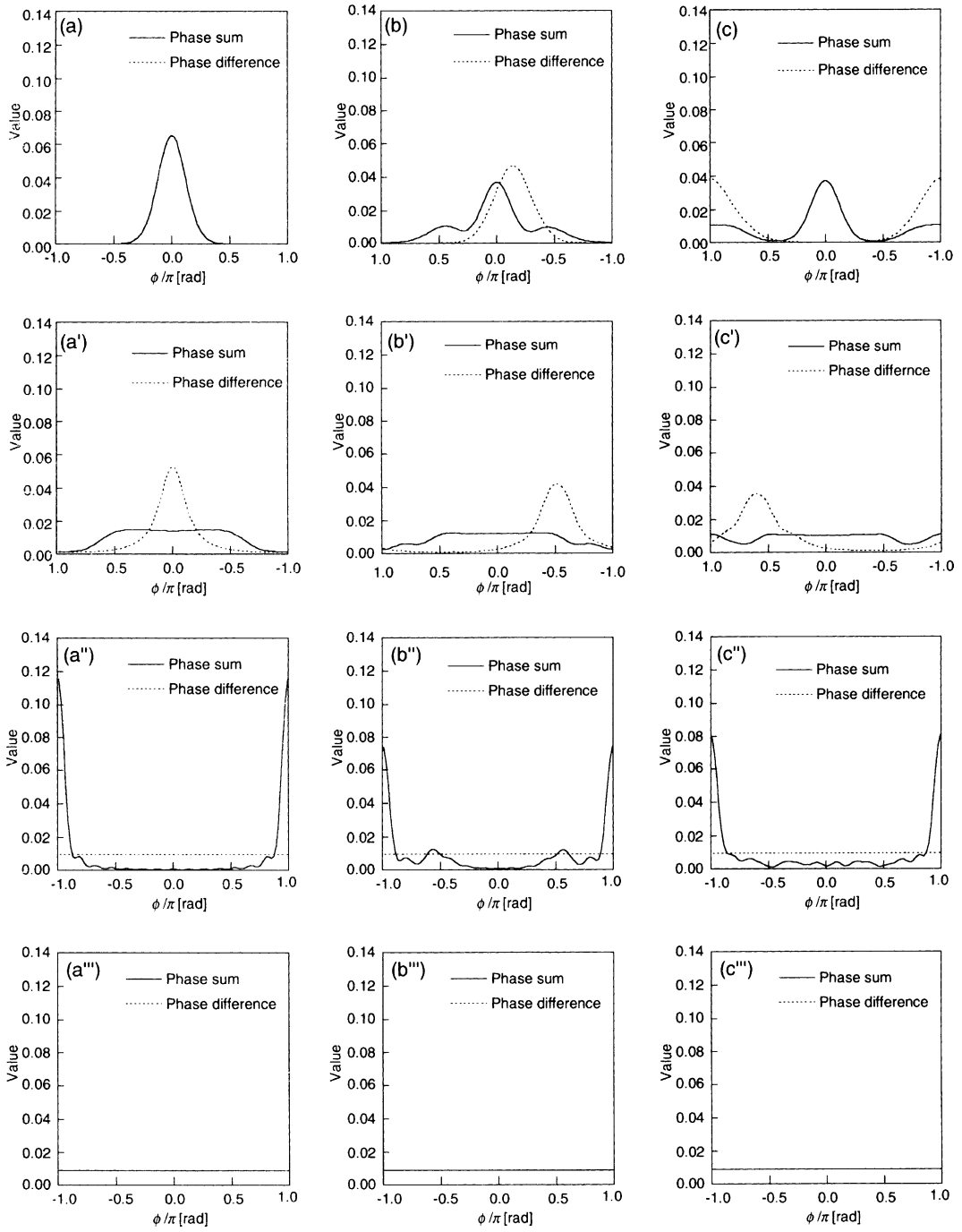

Fig. 3. Photon-phase-sum (solid line) and -difference (dotted line) distributions (represented by $P(\phi^+)$ and $P(\phi^-)$, respectively) of the two-mode coherent (TC), two-mode squeezed coherent (TSC), two-mode squeezed vacuum field (TSV) and two-mode thermal field (TT) at times (a)–(c) for (TC), (a′)–(c′) for (TSC), (a″)–(c″) for (TSV) and (a‴)–(c‴) for (TT) (see Fig. 2).

(TT) exhibit a uniform distribution with a constant value (which means completely random photon phase), so that all the off-diagonal atomic/molecular density matrices for (TT) completely vanish (see Fig. 2(TT-od)).

Finally, we discuss the relation between the present attractive feature in off-diagonal molecular density matrices under a two-mode squeezed vacuum field (TSV) and observed phenomena. Such off-diagonal molecular density matrices, which represent the coherency between molecular states, determine the feature of molecular response properties, e.g., linear and non-linear polarization. To our knowledge, the relation between non-linear optical polarization and two-mode squeezed vacuum is discussed for the first time in this study though there are a few studies that discuss the non-linear optical responses and other quantized fields [25]. The fourth-order optical processes, which describe the third-order non-linear optical phenomena, are characterized by the three types of virtual/real excitation processes. These processes are classified by types of a series of products of transition moments (μ_{ij}) involved in a perturbational formula [24]. Namely, the molecular third-order response properties (the second hyperpolarizabilities) are known to be expressed by the type (I) (**g-e-e-e-g**), type (II) (**g-e-g-e′-g**), type (III-1) (**g-e-e-e′-g**) and type (III-2) (**g-e-e′-e″-g**) (see Fig. 4), where **g** and **e** (**e′** and **e″**) represent the ground and excited states, respectively. For example, the excitation process (**g-e-e-e′-g**) corresponds to the term involving $d_{ge}d_{ee}d_{ee'}d_{e'g}$. These processes exhibit peculiar features of magnitudes, signs and frequency dependencies. The type (I) process provides a positive contribution, while the type (II) does a negative contribution in the first off- and near-resonant region [24]. Although the type (III) contributions have the possibility of taking positive or negative contribution, they usually provide positive contributions in such region. One of the most important results obtained in this study is that the off-diagonal density matrix between states which are resonant with the two-photon ($\omega_1 + \omega_2$) process for a two-mode squeezed vacuum field (TSV) maintains a large value, while all other off-diagonal density matrices completely vanish. This feature is expected to remarkably affect the excitation processes (I)–(III) and thus to provide a significant influence on the third-order response properties though the relation between off-diagonal density matrices and each type of process is generally complicated [26]. As a simple example, we consider a ladder-type three-state model composed of the ground state 1, excited states 2 and 3 ($E_1 < E_2 < E_3$), where only the transition moments of 1–2 and 2–3 states are assumed to exist. Of course, a conventional laser field causes the third-order polarization in this model and its second hyperpolarizability is described by (II) (1–2–1–2–1) and (III-2) (1–2–3–2–1). In contrast, if we apply the two-mode squeezed vacuum field (TSV) with frequencies ω_1 and ω_2, which are resonant with state intervals 1–2 and 2–3, respectively, the second hyperpolarizability disappears. This drastic change can be understood by the fact that the off-diagonal density matrices ($|\rho^{\mathrm{mol}}_{1,2}|$ and $|\rho^{\mathrm{mol}}_{2,3}|$) concerning 1–2 and 2–3 transitions vanish and only $|\rho^{\mathrm{mol}}_{1,3}|$ concerning 1–3 transition exists, while the transition moment d_{13} is equal to 0 in this model. It is speculated for more general state models that the irradiation of two-mode (or more generally n-mode) squeezed vacuum field has the possibility of significantly changing the magnitude (and even signs in some cases) of higher-order hyperpoalrizabilities.

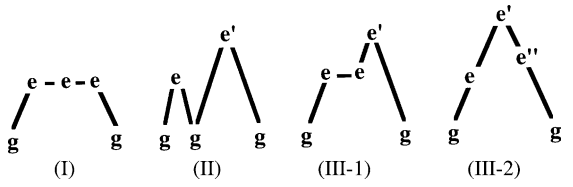

Fig. 4. Three types of excitation processes [24] contributing to second hyperpolarizabilities: type (I) (**g-e-e-e-g**), type (II) (**g-e-g-e′-g**), type (III-1) (**g-e-e-e′-g**) and type (III-2) (**g-e-e′-e″-g**), where **g** and **e** (**e′** and **e″**) represent the molecular ground and excited states, respectively.

4. Conclusion

In this study, we found that although the two-mode squeezed vacuum and two-mode thermal fields lead to similar irregular Rabi oscillations, only the magnitude of off-diagonal atomic/molec-

ular density matrix $|\rho^{\mathrm{mol}}_{1,3}|$ maintains large values in contrast to the disappearance of all the off-diagonal atomic/molecular density matrices for the two-mode thermal field. The two-mode squeezed coherent field with the intermediate squeezing intensity ($r = 1.0$) was found to cause the significant decrease in $|\rho^{\mathrm{mol}}_{1,3}|$ as compared to the case of two-mode coherent field though the collapse-revival behavior of atomic/molecular populations for these two fields is similar to each other. This result indicates that the two-mode squeezed fields directly cause remarkable changes in the relative phase (coherency) between the atomic/molecular states in resonance with the phase-sum frequency of the two-mode field. It is particularly interesting that the two-mode squeezed vacuum field causes the anomalous coherency between atomic/molecular states, where both the thermal ($|\rho^{\mathrm{mol}}_{1,2}| = |\rho^{\mathrm{mol}}_{2,3}| = 0$) and the quantum-coherence ($|\rho^{\mathrm{mol}}_{1,3}| \neq 0$) features coexist during the dynamics though the atomic/molecular populations for that field provide similar irregular Rabi oscillations to those for the two-mode thermal field. As we predicted the effects of a two-mode squeezed vacuum field on the non-linear response properties, such attractive features in the dynamics of the off-diagonal atomic/molecular density matrices for two-mode squeezed fields will be useful for the direct manipulation of the atomic/molecular electronic coherency.

Acknowledgements

This work was supported by Grant-in-Aid for Scientific Research (No. 14340184) from Japan Society for the Promotion of Science (JSPS) and a Grant from the Ogasawara Foundation for the Promotion and Science & Engineering.

References

[1] M. Nakano, K. Yamaguchi, Chem. Phys. 252 (2000) 115.
[2] M. Nakano, K. Yamaguchi, J. Phys. Chem. 103 (1999) 6036.
[3] M. Nakano, K. Yamaguchi, J. Chem. Phys. 112 (2000) 2769.
[4] M. Nakano, K. Yamaguchi, Chem. Phys. Lett. 317 (2000) 103.
[5] E.T. Jaynes, F.W. Cummings, Proc. IEEE 51 (1963) 100.
[6] B.W. Shore, P.L. Knight, J. Mod. Opt. 40 (1993) 1195.
[7] M. Brune, F. Schmidt-Kaler, A. Maali, J. Dreyer, E. Hagley, J.M. Raimond, S. Haroche, Phys. Rev. Lett. 76 (1996) 1800.
[8] D.M. Meekhof, C. Monroe, B.E. King, W.M. Itano, D.J. Wineland, Phys. Rev. Lett. 76 (1996) 1796.
[9] V. Buzek, T. Quang, J. Opt. Soc. Am. B 6 (1989) 2447.
[10] W.K. Lai, V. Buzek, P.L. Knight, Phys. Rev. A 44 (1991) 6043.
[11] R. Loudon, P.L. Knight, J. Mod. Opt. 34 (1987) 709.
[12] S.M. Barnett, P.L. Knight, J. Opt. Soc. Am. B 2 (1985) 467.
[13] D.T. Pegg, S.M. Barnett, Phys. Rev. A 38 (1989) 1665.
[14] Z.G. Soos, S.J. Ramasesha, Chem. Phys. 90 (1989) 1067.
[15] C.M. Caves, B.L. Schumaker, Phys. Rev. A 31 (1985) 3068.
[16] B.L. Schumaker, C.M. Caves, Phys. Rev. A 31 (1985) 3093.
[17] A.K. Ekert, P.L. Knight, Am. J. Phys. 57 (1989) 692.
[18] C.T. Lee, Phys. Rev. A 42 (1990) 4193.
[19] C.M. Caves, C. Zhu, G.J. Milburn, W. Schleich, Phys. Rev. A 43 (1991) 3854.
[20] M. Selvadoray, M. Sanjary Kumar, R. Simon, Phys. Rev. A 49 (1994) 4957.
[21] S.M. Barnett, D.T. Pegg, J. Mod. Opt. 44 (1997) 225.
[22] J. Eiselt, H. Risken, Phys. Rev. A 43 (1991) 346.
[23] M.J. Werner, H. Risken, Phys. Rev. A 44 (1991) 4623.
[24] M. Nakano, K. Yamaguchi, Phys. Rev. A 50 (1994) 2989.
[25] N.Ph. Georgiades, E.S. Polzik, H.J. Kimble, Phys. Rev. A 59 (1999) 676.
[26] M. Nakano, K. Yamaguchi, Chem. Phys. Lett. 356 (2002) 462.